Laser Physics, Vol. 12, No. 4, 2002, pp. 729–735.

Light-Induced Decoherence in the Driven Evolution of an Atom

Chr. Balzer, Th. Hannemann, D. Reiss, W. Neuhauser, P. E. Toschek, and Chr. Wunderlich

Institut für Laser-Physik, Universität Hamburg, Jungius-Str. 9, Hamburg, D-20355 Germany

e-mail: toschek@physnet.uni-hamburg.de

Received September 24, 2001

Abstract—Atoms or ions prepared in traps for applications in quantum information processing (QIP) often become addressed by radiation within schemes of alternating microwave-optical double resonance. QIP requires thorough assessment of decoherence. A well-defined amount of decoherence may be applied to the system when spurious resonance light is admitted simultaneously with the driving radiation. This decoherence is quantified in terms of longitudinal and transversal relaxation. It may serve for calibrating observed decoherence as well as for testing error-correcting quantum codes.

Spectroscopy on individually prepared atomic particles has twofold motivation:

—the investigation of single-particle effects unobservable in ensembles and

—tests of the particle's conditions supposed to meet the requirements of negligible perturbation: that is, the needs of frequency standards, or of quantum information processing (QIP).

In both respects, *quantum decoherence* plays an important role, i.e., the disturbing intervention imposed upon the phase of the system's quantum state by the environment or the meter. It is the purpose of this contribution to report upon the design of well-defined decoherence on such a quantum systems that may be useful for tests of either the system, or of the manipulative procedures performed upon it. Spectroscopic techniques that are most appropriate for dealing with an individual quantum system [1] are certain schemes of "double resonance" detection whose details may vary. The radiation driving the dynamics on a principal resonance (a hyperfine or electronic one) may be a radiowave, a microwave, or laser light, whereas additional probe light excites scattering on a resonance line as manifestation of the atom being found in one particular of the two states of the principal resonance. Often, it is not suitable to use cw drive and probe fields of radiation, or to simultaneously apply pulses of these radiations, in order to avoid the complications of light shift and dynamic Stark effect. There are two basic strategies: (1) Single driving pulses alternating with probe pulses, which is sometimes called "Rabi's scheme" and (2) double pulses separated by free evolution, and succeeded by probing, a strategy that transposes Ramsey's method for a molecular beam's resonance excitation to the time domain, extending this spectroscopic technique into interferometry.

An example of the former approach with laser pulses driving an electronic transition—preferentially a dipole-forbidden one—is shown in Fig. 1. A drive pulse and a probe pulse make up for preparation and measurement of the quantum system that is being found either in state O (probe-excited light scattering on) or in state 1 (light scattering off) [2]. This is considered an "observation." Note that a time series of many subsequent observations—a "trajectory" that looks like a "random telegraph signal"—includes correlations of various orders between the individual observations. As an example, let us consider two subsequent results. The number of "on"–"off" pairs, normalized to the number of "on" results, directly yields the probability of absorption of the driving light (and excitation of the ion), the number of "off"–"on" pairs that re-emission (and deexcitation of the ion) (Fig. 2).

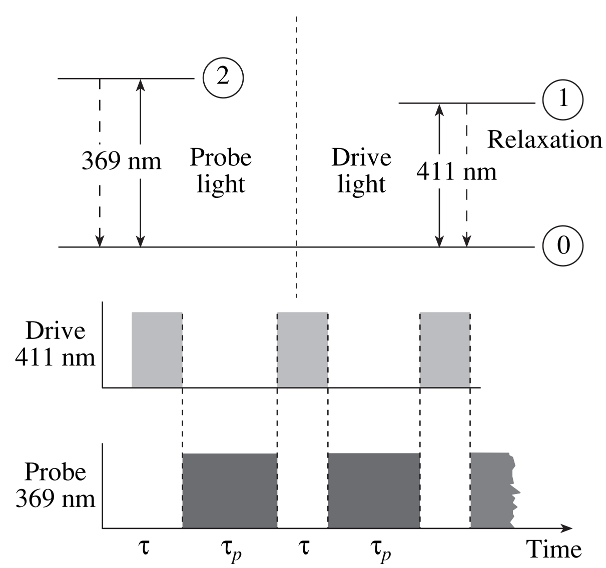

Fig. 1. Double-resonance addressing of individual atoms by alternating drive and laser probe pulses that excite resonance scattering to be detected. Here the driving pulses are laser light, and the wavelengths correspond to the ion $^{172}Yb^+$.

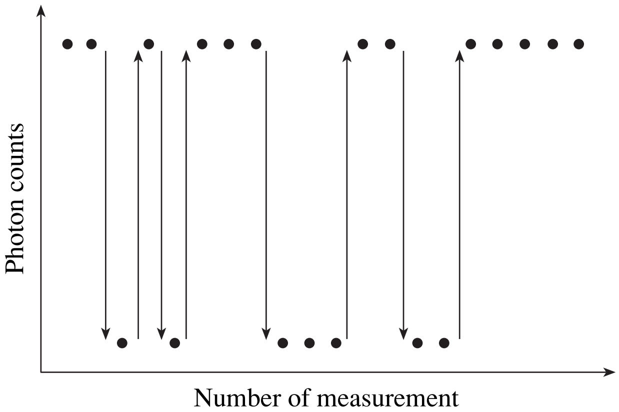

Fig. 2. Trajectory of the results (light scattering "on" or "off") of subsequent individual measurements. On-off pairs. represent excitation (of the atom) and absorption (of the drive radiation), off-on pairs de-excitation and emission.

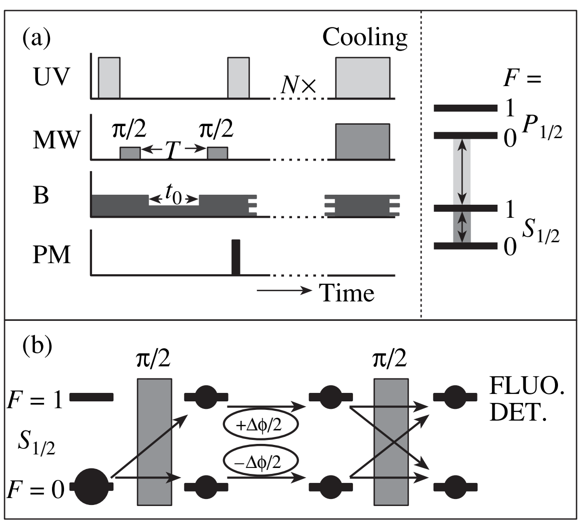

Fig. 3. Gating scenario of double-pulse driving by microwave (MW), UV probing, switching of magnetic field B, and detection of scattered light (PM), and simplified level scheme of atom (top). Interpretation as atomic-wave Mach–Zehnder interferometer in configuration space (bottom). The beam splitters are represented by the two $\pi/2$ driving pulses.

Averaging over the results of a trajectory yields the expectation value of the pulse-driven attempts of excitation, based on an *ensemble of measurements*. However, unlike with an ensemble of systems, the microstate of *this* ensemble is completely known from the detected trajectories, including all correlations between individual measurements. Thus, the corresponding observable of the individual system is completely controlled, and this very fact leaves the system suitable for applications in QIP [3].

For an illustration of the second approach, let us consider microwave-optical double-resonance spectroscopy on the ground-state hyperfine resonance of an ion that employs two temporally separated driving pulses with each observation, succeeded by a probe pulse (Fig. 3) [4]. When incrementing the driving frequency, or the pulse separation, upon each subsequent measurement, the trajectories again seem random sequences of "on" and "off" results, although they are correlated with the temporally advancing phase of the observed system. A superposition of many trajectories consequently reveals fringes that document the interference of the ion's two pathways of evolution, between the $\pi/2$ driving pulses, via the $F = 0$ or the $F = 1$ state. A difference of the phases of spin precession that have accumulated, during the time of the $\pi/2$-pulse separation, to values that are *different* along the two paths of evolution shows up as a shift of the fringe pattern (Fig. 4) [4]. Thus, this approach qualifies as atom interferometry in configuration space.

A small number of ions prepared in an electrodynamic or electromagnetic trap, laser-cooled and individually addressed according to the above or more complex strategies indeed represent, with some of their internal or motional resonances, a specific number of "qubits," the elements for the storage and processing of quantum information [3]. In fact, they represent a scalable system, in contrast with certain competitive approaches, as, e.g., spin resonance spectroscopy on large molecules [5]. The more important is the realization and full understanding of the radiative interactions of such a system: The implementation of coherent dynamics of an individual atomic particle being radiatively driven is prerequisite for the operation of any quantum-logical gate, in particular of the basic Hadamard transformation [6]. The demonstration of coherently controlled dynamics of trapped ions has been reported on the first vibrational sidebands (or "one-phonon lines"), and on the carrier ("zero-phonon") line of a laser-driven Raman transition between ground-state hyperfine levels [7], with a microwave-driven hyperfine carrier line [4], with the vibrational sidebands of a dipole-forbidden optical line [8], and with a corresponding optical carrier line [9]. Some of these schemes are ridden by imperfectly identified kinds of decoherence that would thwart the performance of a substantial number of successive steps of coherent interaction. This decoherence may range from the residual decay of the involved metastable states to spurious light scattering, and to phase fluctuations of the applied radiation. For instance, the decoherence on the vibrational dynamics of ions localized in a Paul trap [6] has been suggested recently to result from parasitic spontaneous scattering of the two off-resonant light fields that served as pump and Stokes waves for Raman excitation of the hyperfine resonance [10]. Also, various types of reservoirs have been implemented that make decay the specific motional states in characteristic ways [11].

We have found, in a microwave-optical double-resonance experiment, decoherence to appear on the coherent spin evolution of an individual trapped and cooled $^{171}Yb^+$ ion, microwave-driven on the ground-state hyperfine transition. The observed decoherence was brought about by a minute amount of residual laser light that impinged upon the ion while the microwave drive was applied. Blocking out this spurious light completely eliminated the decoherence. We are going to show that well-defined quantities of longitudinal and transversal relaxation may be admitted to the ion by controlling the strength and polarization of the light, and the level and direction of the ambient magnetic field. Such a "designed" decoherence seems useful for the quantitative estimate of observed decoherence, and as a testing ground both for the sensitivity of quantum algorithms to the action of decoherence as well as for the function of error-correcting codes.

The double-resonance experiment was performed on a single $^{171}Yb^+$ ion in a 2-mm-sized electrodynamic trap. The $F = 0 \longrightarrow 1$ hyperfine resonance of the ion's $S_{1/2}$ ground state was driven, for $\delta t = 100$ or 400 μs, by 12.6-GHz microwave radiation. Probing the $F = 1$ state immediately followed, when the ion was shone by a 5-ms pulse of 369-nm laser light. The excitation and observation of resonance scattering on the $S_{1/2}(F = 1) \longrightarrow P_{1/2}(F = 0)$ line proved successful the preceding attempt of microwave excitation; the absence of scattering proved this attempt to have failed. A frequency-doubled Ti: sapphire laser generated 369-nm light of about 100 kHz bandwidth. This light, down-tuned from resonance by 10 MHz, was scattered on the ion's $S_{1/2}$–$P_{1/2}$ resonance line, such that the ion was cooled deep into the Lamb–Dicke regime. Occasional optical pumping of the ion into its metastable $D_{3/2}$ level was counteracted, when 935-nm light of a diode laser re-pumped the ion into the ground state. Trajectories of individual measurements were recorded, each of which includes an initial preparatory light pulse that pumps the ion into state $F = 0$, a microwave driving pulse of length $\tau = N\delta t$, a probe-light pulse, and simultaneous recording of the presumptive fluorescence scattered off the ion (Fig. 5). Within a set of measurements making up a trajectory, N varied from 1, indicating the initial measurement, through 300, the final one. The recorded signals form quasi-random sequences of "on" and "off" results; however, the superposition of many accumulated trajectories yields the probability $P_1(\theta)$ for occupation of the $F = 1$ hyperfine component of the ground state by the ion, as a function of the driving time τ. The data of 50 trajectories were superimposed, and modulation of P_1 emerges that is ascribed to Rabi nutation of the ion driven by the microwave pulses of area $\theta = \Omega\tau$, whose duration τ was stepwise extended (Fig. 5, bottom).

The nutational oscillation shows high contrast. However, when a spurious level of probe light is admitted to the ion *simultaneously* with the driving pulses, the evolution of the probability of light scattering is dramatically modified (Fig. 6a): (i) The Rabi nutation becomes damped with its time constant shortened upon increased intensity of the background light. (ii) At long times τ, the probability $P_1(\theta)$ saturates to a level somewhere between one half and unity, and not necessarily to level 1/2.

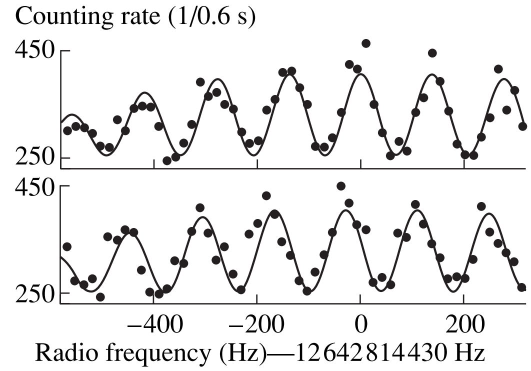

Fig. 4. Photo counting rate of single-ion fluorescence vs micro-wave detuning. Each data point shows accumulated results of 300 attempts; dc magnetic field B_0 constant (top), and set to $B_0 - \Delta B$ during t_0 yielding the phase shift of fringes $\langle\Delta\phi\rangle = 1.28$ rad. (From [4].)

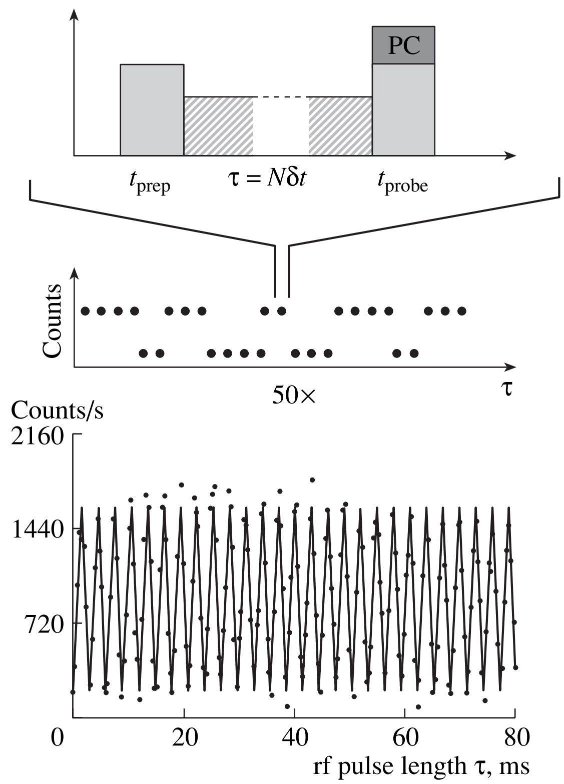

Fig. 5. An individual measurement includes a pulse of resonant light that prepares the ion in the $F = 0$ state of the ground-state hyperfine doublet, a microwave driving pulse that is N times a unit length δt, and a probe light pulse. The scattered light is detected by a photon counting (PC) system (top). With each subsequent measurement, N is incremented by a unit, up to N_{max} and yields a sequence of N_{max} data, "on" or "off" (middle). Accumulation of 50 sequences reveals rf nutation on the ground-state hyperfine transition.

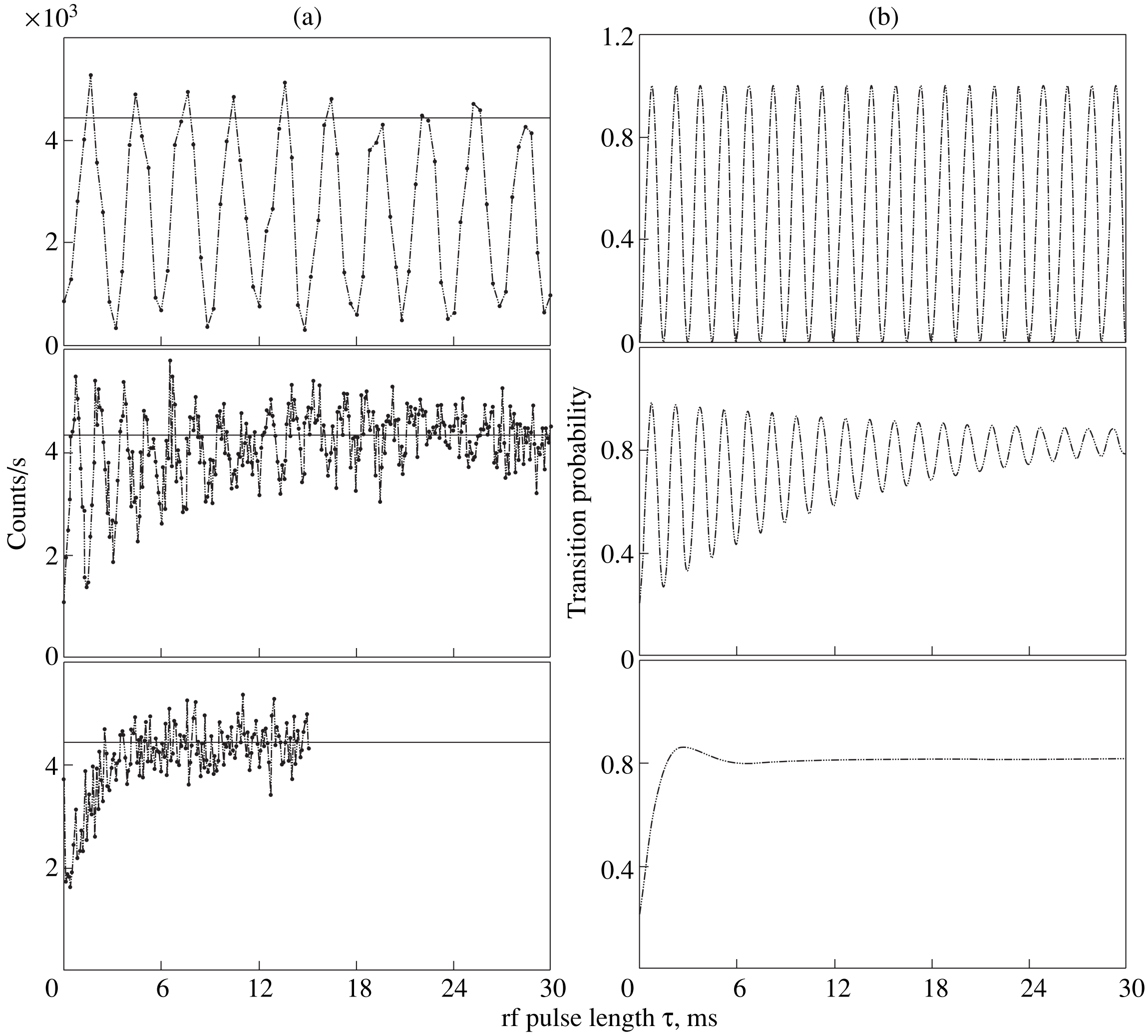

Fig. 6. Scattered-light response vs. length of microwave driving pulse. (a) Observed, with level of light applied to the ion *during* the drive: no light (top), 2 nW (middle), 20 nW (bottom). (b) Simulated: Rabi frequency $\Omega_L = 0$ kHz (top), 50 kHz (middle), 500 kHz (bottom).

In order to account for these observations, the ion, the light fields, and their interaction have been modeled by four-level Bloch equations (Fig. 6b). The corresponding level scheme is shown in Fig. 7. The Zeeman sublevels $m_F = +1$ and -1 have been combined and make up for the effective level 2 not affected by the driving microwave radiation on the hyperfine transition 0–1, with $\Delta m_F = 0$.

The minute light intensity applied to the ion during the driving intervals is far below saturation of the resonance line, $I = \Omega_L^2/\gamma_l\Gamma_3 \ll 1$, where Ω_L is the Rabi frequency of the ion generated by the laser light, Γ_3 and $\gamma_l = \Gamma_3/2 + \gamma_{lph}$ are the rate constants of energy relaxation of the resonance level ($P_{1/2}$) and of phase relaxation of the laser-excited (electric) dipole, respectively. In the present experiment, the extra rate of phase relaxation is small, $\gamma_{lph} \ll \Gamma_3$ and it is neglected. In the above limit, it is appropriate, for the interpretation of the ionic evolution, to restrict the modeling of the *optical* part of the dynamics, i.e., the part related to the three levels 1, 2, 3 and their connecting transitions, to optical pumping and decay, in terms of rate equations. This rate evolution is coupled to the microwave-driven coherent evolution, on the resonance 0–1, via level 1 that represents state $S_{1/2}(F = 1, m_F = 0)$. Now, the latter two-level dynamics appears affected by light-generated decoherence of two kinds: (i) A net loss of population, from the driven two-level system 0–1, by optically pumping the ion into state 2, i.e., into the $F = 1$ Zeeman sublevels $m_F = \pm 1$, with subsequent re-pumping, and (ii) additional loss of phase coherence of the driven spin dynamics by Rayleigh scattering in the eigenstate 1, i.e., $F = 1$, $m_F = 0$.

The loss of some population from state 1 to state 2 makes the probability P_1 of finding the ion in the entire probed hyperfine state $F = 1$ (states 1 and 2) saturate *above* 1/2, since the Zeeman sublevels ±1 (state 2) retain part of the population from being coherently transferred—on the condition $\Delta m_F = 0$—into state $F = 0$. This fractional population of state 2 may become re-excited, however, by a component of the linearly polarized laser light and taken back to state 1 ($F = 1$, $m_F = 0$), during the intervals of probing, since the width of the resonance line far exceeds the small Zeeman splitting of the $S_{1/2}(F = 1)$ state. Complete pumping to level 2 ($m_F = \pm1$) makes P_1 saturate at unity. The scattering rates are $\beta_f n_i r_i$, where n_i is the population in the initial state, β_f is the branching ratio of the decay of state 3 into the final state ($\beta_1 = \frac{1}{3}$, $\beta_2 = \frac{2}{3}$), and the scattering rate per atom is the average population $\langle P_3\rangle$ of state 3, times the decay rate Γ_3, such that

$$r_1 = \langle P_3(0)\rangle\Gamma_3, \tag{1}$$

and

$$r_2 = (\langle P_3(+1)\rangle + \langle P_3(-1)\rangle)\Gamma_3. \tag{2}$$

Here ($m \equiv m_F$),

$$\langle P_3(m)\rangle = \frac{1}{2}\frac{I(m)\mathfrak{L}(B, m)}{1 + I(m)\mathfrak{L}(B, m)}, \tag{3}$$

where $I(\pm1) = I_0\sin^2\alpha$, $I(0) = I_0\cos^2\alpha$, I_0 is the density of light flux at the ion's location, α is the angle subtended by light polarization and magnetic field B,

$$\mathfrak{L}(B, m) = \frac{(\Gamma_3/2)^2}{(\Gamma_3/2)^2 + (\omega_0 - \omega + m\delta)^2},$$

ω and ω_0 are the light and resonance frequencies, respectively, $\delta = g_F\mu_B B/\hbar$, $g_F \simeq 1$ is the Landé factor of state 2, and μ_B Bohr's magneton [12]. Now, let us further restrict the model to the two-level system that consists of states 0 and 1, and attribute to it conventional rates per atom of phase and energy relaxation, γ and Γ respectively. For such a model, a closed solution is available [13]. The dynamics of its population includes damped nutational oscillation and some offset of the upper-state probability that exponentially decays (on resonance) to a saturating level $P_1^{(2)} = \frac{1}{2}\frac{I}{1+I}$, where $I = \Omega^2/\Gamma\gamma$ and Ω are intensity and Rabi frequency of the microwave, respectively (Fig. 8). The rate constants γ and Γ will become *identified* with quantities taken from the above three-level model: The spin nutation gives rise to oscillation of the population difference in the two-level system that is supposed to damp out exponentially with the effective constant γ of phase relaxation, such that

$$\gamma = \frac{\Gamma}{2} + \gamma_{ph} \mathrel{\hat{=}} r_1, \tag{4}$$

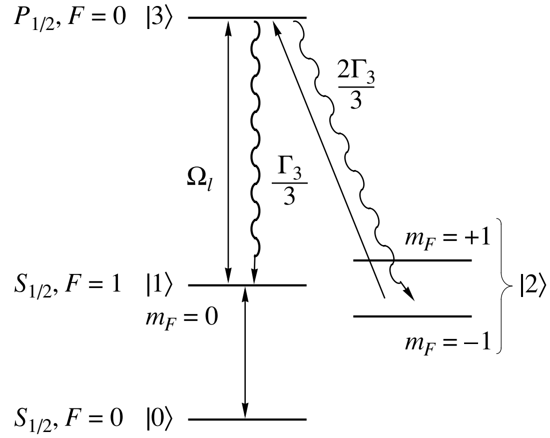

Fig. 7. Simplified level scheme of the $^{171}Yb^+$ ion used in the described microwave-optical double resonance experiment.

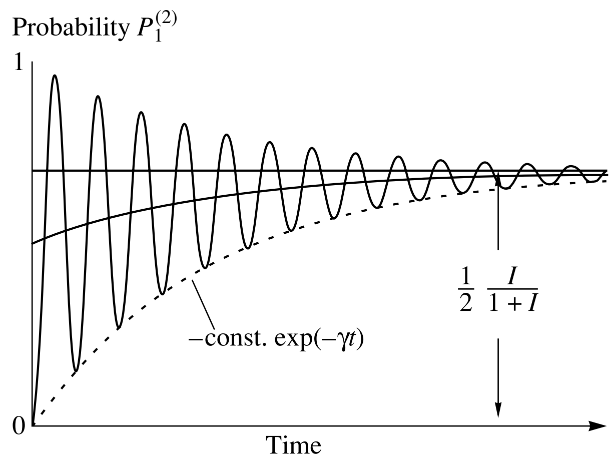

Fig. 8. Probability of upper-state (l) population, vs. time, of a relaxing atomic two-level system [13]. The evolution is characterized by the decay of the nutational oscillation (γ), and by level of saturation determined by $I = \Omega^2/\Gamma\gamma$.

where γ_{ph} is the contribution of extra phase perturbation not related to intrinsic relaxation. Moreover, the flow equilibrium established by the scattering as well as the quasi-steady state on the microwave-driven line require

$$n_0 = n_1 = \frac{1 - n_2}{2} \tag{5}$$

and

$$\frac{1}{3}n_2 r_2 = \frac{2}{3}n_1 r_1. \tag{6}$$

Thus, $n_2 = \frac{r_1}{r_1 + r_2}$, and the normalized probe signal, i.e., the probability of finding the system in one of states 1 or 2 of the 3-level system, corresponding to the

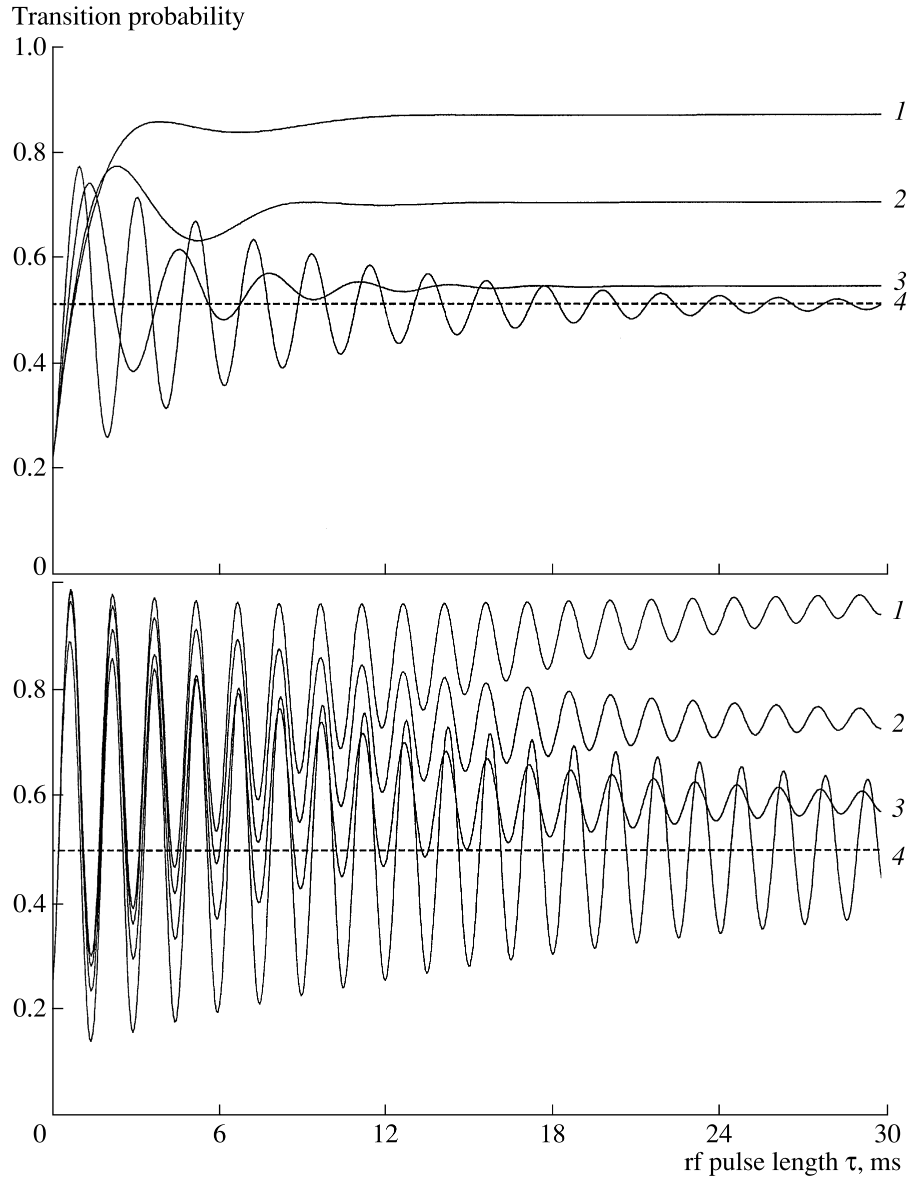

Fig. 9. Probability $P_1(\theta)$ of the ion to be found in the upper state 1 after having been driven by a microwave pulse of area $\theta = \Omega\tau$. Weak resonance scattering excited by laser light of intensity $I = \Omega_L^2/\Gamma_3\gamma_l$ mimics phase relaxation and energy decay into state 1. Initial population in 0: 0.8, in 1: 0.2. Detuning $\delta = -0.28$, $\delta_l = -3 \times 10^3$. $\Gamma_3 = 18 \times 10^3$, $\Omega = 4.2$. Top: $\sqrt{2r_1\gamma_l} = 700$, $\sqrt{r_2\gamma_l} = 70$ (*1*), 140 (*2*), 350 (*3*), 700 (*4*). Bottom $\sqrt{2r_1\gamma_l} = 70$, $\sqrt{r_2\gamma_l} = 7$ (*1*), 70 (*2*), 140 (*3*), 350 (*4*). All frequencies in $2\pi \times$ kHz.

upper state 1 of a driven and decaying two-level system, is

$$\begin{aligned} P_1^{(3)} &= n_1 + n_2 = \frac{1+n_2}{2} \\ &= 1 - \frac{1}{2}\frac{r_2/r_1}{1+r_2/r_1} \\ &= 1 - P_0^{(3)}. \end{aligned} \tag{7}$$

One may identify $P_0^{(3)}$ with the effective two-level excitation probability $P_1^{(2)}$. This interpretation (i) yields the effective rate constant of energy relaxation,

$$\Gamma \mathrel{\hat{=}} \frac{\Omega}{r_2}, \tag{8}$$

and (ii) shows that this effective relaxation makes the ion decay into the *excited* state 1. Note that the two effective rate constants γ and Γ of Eqs. (4) and (8) may be set *separately* by suitable selection of the light polarization and/or of the ambient magnetic field. Figure 9 shows trajectories calculated with selected values of $T_0 = \Gamma^{-1}$ and $T_2 = \gamma^{-1}$. They demonstrate various degrees of damping as well as different levels of saturation of $P_1(\tau)$.

With a single atom competing pathways of spontaneous decay into non-degenerate levels may generate correlation of the final states in the atom [14]. Therefore, complete modeling of the rate of optical pumping represented by Eq. (2) would require one to include an interference term of the transition amplitudes of the back-and-forth optical pumping, via the states $F = 1$, $m_F = +1$ and -1, that give rise to indiscernible pathways. This term displays a resonance in zero magnetic field and represents what is called "zero-field level crossing" [15], a ground-state Hanle effect. The width of the crossing resonance is determined by the lifetime of the intermediate interfering states. The $F = 1$ levels show an effective lifetime on the order of milliseconds, or longer. Thus, the interference term in rate r_2 would make vary this rate across a spectral tuning range of the laser less than 1 kHz wide. This spectral feature is not resolved by the emission bandwidth of the laser.

The availability of easily quantifiable longitudinal and transversal relaxation that is *light-induced* upon individual atomic systems displays important advantages when it comes to the application of such a system to manipulations in QIP impaired by loss of coherence. In particular, codes of information processing may be tested for their applicability under this challenging but common-place condition. On the other hand, codes for error correction may be made to demonstrate their capacity upon increasing levels of decoherence fed into the system. The light-induced decoherence, as demonstrated in this report, is readily applicable to various strategies of individually addressing quantum systems by various schemes of optical double-resonance detection. This decoherence may be switched on and off immediately, and it is reproducible.

In summary, a simple method has been outlined that adds a predetermined degree of decoherence on the coherent radiative interaction of an individual atom or ion that is considered to carry quantum information. Although, in the reported experiment, the coherent drive was microwave radiation resonant with a ground-state hyperfine transition. the same principle seems applicable to systems where a dipole-forbidden optical transition is driven by laser light.

This work was supported by the Hamburgische wissenschaftliche Stiftung.

REFERENCES

1. Toschek, P.E., 1982, Atomic Particles in Traps, Les Houches Session 1982, *New Trends in Atomic Physics*, Grynberg, G. and Stora, R., Eds. (Amsterdam: North-Holland), p. 383.
2. Appasamy, B., Siemers, I., Stalgies, Y., Eschner, J., Blatt, R., Neuhauser, W., and Toschek, P.E., 1995, *Appl. Phys. B*, **60**, 473.
3. See, e.g., Steane, A., 1997, *Appl. Phys. B*, **64**, 623.
4. Huesmann, R., Balzer, Ch., Courteille, Ph., Neuhauser, W., and Toschek, P.E., 1999, *Phys. Rev. Lett.*, **82**, 1611.
5. See, e.g., Jones, J.A., 2000, *Fortschr. Phys.*, **48**, 909.
6. Meekhof, D.M., Monroe, C., King, B.E., Itano, W.M., and Wineland, D.J., 1996, *Phys. Rev. Lett.*, **76**, 1796.
7. Monroe, C., Meekhof, D.M., King, B.E., Itano, W.M., and Wineland, D.J., 1995, *Phys. Rev. Lett.*, **75**, 4714.
8. Appasamy, B., Stalgies, Y., and Toschek, P.E., 1998, *Phys. Rev. Lett.*, **80**, 2805; Roos, Ch., Zeiger, Th., Rohde, H., Nägerl, H.C., Eschner, J., Leibfried, D., Schmidt-Kaler, F., and Blatt, R., 1999, *Phys. Rev. Lett.*, **83**, 4713.
9. Balzer, Ch., Huesmann, R., Neuhauser, W., and Toschek, P.E., 2000, *Opt. Commun.*, **180**, 115.
10. Di Fidio, C. and Vogel, W., 2000, *Phys. Rev. A*, **62**, 031802-1.
11. Turchette, Q.A., Myatt, C.J., King, B.E., Sackett, C.A., Kielpinski, D., Itano, W.M., Monroe, C., and Wineland, D.J., 2000, *Phys. Rev. A*, **62**, 053807.
12. Meystre, P. and Sargent III, M., 1990, *Elements of Quantum Optics* (Berlin: Springer), sect. 15.
13. Torrey, H.C., 1949, *Phys. Rev.*, **76**, 1059.
14. Schubert, M., Siemers, I., Blatt, R., Neuhauser, W., and Toschek, P.E., 1995, *Phys. Rev. A*, **52**, 2994.
15. See, e.g., Haken, H. and Wolf, H.C., 1990, *Atom- und Quantenphysik* (Berlin: Springer).